Effect of the contact area on sliding velocity

K. Arakawa
Research Institute for Applied Mechanics,
Kyushu University, Japan

Abstract

In this study, we investigated the sliding friction of Teflon (polytetrafluoro-ethylene: PTFE) samples on an inclined glass plate with a smooth transparent surface. The sliding velocity and contact area of the samples were evaluated as functions of the sliding length and inclined angle, and their relationships were determined to examine the effect of the contact area on the sliding velocity. Our results showed that the velocity decreased as the contact area increased, due to the wear of the samples, suggesting that the contact area plays an important role in sliding friction.
Keywords: Teflon, glass, sliding friction, sliding velocity, contact area, wear.

1 Introduction

Friction is one of the most significant physical phenomena observed in daily life, and thus has been studied since ancient times to elucidate the frictional forces acting at the interface between two solids. For the static case, it is well established that the frictional force F is given by $F = \mu N$, where μ is the coefficient of friction, and N is the contact force at the interface. This equation indicates that F is proportional to N and is independent of the apparent contact area. For the dynamic case, however, many aspects of friction are still not well understood. Therefore, the dynamic contact between two sliding solids has been widely studied both analytically and experimentally across various disciplines at the nano- and macroscale [1–4]. Nanoscale investigations over the last decade have shown that factors including the contact force [5–10], contact area [11–15], sliding velocity [7, 8, 10, 16–19], surface roughness [11], temperature [20, 21], humidity [16, 18, 22], and wear [6, 23] of the interface are important factors for dynamic friction. However, these effects are not well understood to date.

WIT Transactions on Engineering Sciences, Vol 91, © 2015 WIT Press
www.witpress.com, ISSN 1743-3533 (on-line)
doi:10.2495/SECM150021

In a previous study [24], we investigated dynamic friction during the oblique impact of a golf ball, by evaluating the ball's angular velocity, the contact force, and the contact area between the ball and a target. The effect of the contact area on the angular velocity was evaluated, and our results indicated that the contact area plays an important role in dynamic friction. We suggested that the dynamic frictional force F is given by $F = \mu N + \mu\eta\, dA/dt$, where dA/dt is the time derivative of the contact area A, and η is a coefficient associated with the contact area.

In this study, we investigated the sliding behaviour of Teflon samples on an inclined glass plate with a smooth transparent surface, using a video camera. The video images were used to measure the sliding length of the samples as a function of time to determine their sliding velocities. The contact area between the sample and the glass plate was measured to examine the effect of the contact area on the sliding velocity.

2 Methods

Figure 1 shows the test samples for this experiment. The contact surfaces between the sample and the glass plate consisted of three spheres of Teflon (Flonchemical Co., Japan) attached tightly to a steel disk (outer diameter: 90 mm; inner diameter: 20 mm; thickness: 9 mm). Two different sizes of the spheres were used to vary the contact area; their diameters were 9.52 mm (3/8 in) for Sample 1 and 19.05 mm (3/4 in) for Sample 2. Polycarbonate (PC) sockets were used for Sample 1 to hold the spheres tightly and prevent rotation. The mass of both samples was 410 g. The contact surfaces were cleaned with ethanol before each experiment.

Figure 2 shows the sliding-test and contact-area measurement on a glass plate at an inclined angle of θ. A smooth transparent glass plate (size: 0.3 × 0.9 m^2; thickness: 5 mm) was mounted on a rigid wooden frame to avoid bending and torsion of the plate. Scale marks were glued on the backside of the glass plate to determine the sliding length of the samples. The glass surface was degreased with ethanol; dust and wear particles were removed using a duster made of polyethylene fibres just before each test. The sliding behaviour was recorded using a video

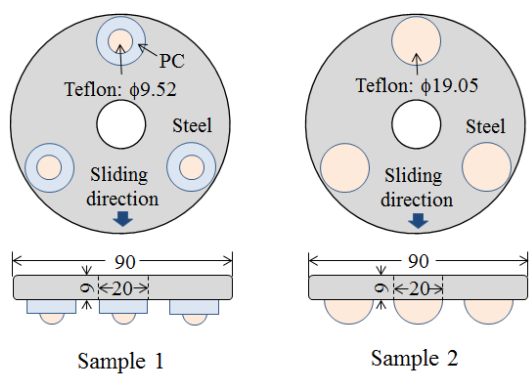

Figure 1: Test samples for the sliding experiment.

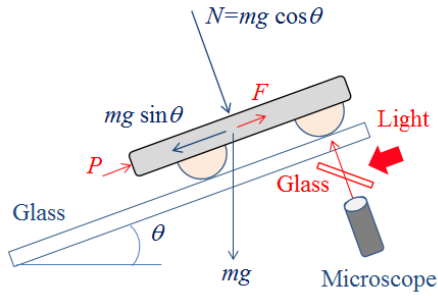

Figure 2: Sliding test and contact area measurement.

camera (Handycam HDR-PJ 760V, Sony Corp.), and the sliding lengths were determined from the still pictures using an image converter (PlayMemories, Sony Corp.). The glass plate was inclined at an angle of $10 < \theta < 20°$. The experiment was conducted at room temperature (i.e., ~22°C) and a relative humidity of ~40%.

The contact area was measured under static conditions, as shown in Fig. 2. The sample was mounted on an inclined glass plate with a point force. The contact surface was illuminated perpendicularly with diffusion light from the backside of the glass plate by inserting a small glass plate (size: 12 × 25 mm^2; thickness: 1 mm). The dark spots resulting from diffuse reflection were recorded at 200× magnification using a digital microscope (MJ-302, Sato Shouji Inc., Japan). The contact area was evaluated from the diameter of the dark spots [24]. We changed the sliding lengths of the samples and measured the contact areas using the procedure described above. The roughness of the contact surfaces was also measured at 1250× magnification using a surface profile microscope (VF-7500, Keyence Inc.).

3 Results and discussion

Figure 3 shows the sliding length L as a function of time t at an inclined angle $\theta = 15°$. L for the two samples increased almost linearly with t except the initial stages of sliding due to the acceleration process of the samples. The slope for Sample 2 was smaller than that for Sample 1 for a given t. The $L-t$ curves determined experimentally were quite different from the theoretical ones given by $F = \mu N$, because L is proportional to the square of time, i.e., $L = 1/2\ (g \sin\theta - \mu N/m)t^2$, where m is the mass of the sample, and g is the gravitational acceleration. This suggests that frictional force is not constant during sliding, and can be related to several factors, including the contact area and sliding velocity.

To minimize data scattering in the evaluation of the sliding velocity, we used a data-fitting procedure based on the least-squares method using the software package Mathematica (Wolfram Research Inc.). Measured values of L were expressed as a seventh-order polynomial of t to fit the observed values (Fig. 3). The sliding velocity v was determined from the first time derivative of the fitted curve $L(t)$ [24].

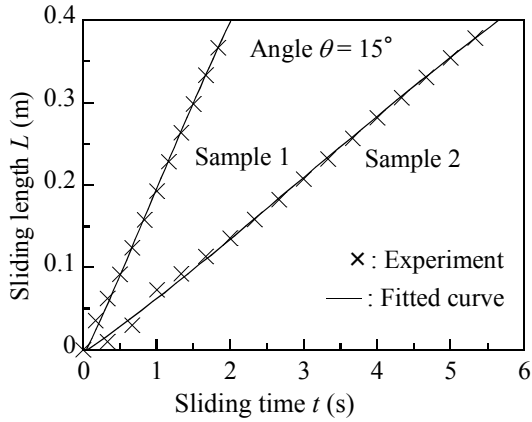

Figure 3: Sliding length L as a function of time t ($\theta = 15°$).

Figure 4 shows v as a function of L at $\theta = 15°$; v for the two samples increased in the early stages of sliding and then slightly decreased in the later stages. The maximum value of v was ~0.2 m/s for Sample 1 and ~0.07 m/s for Sample 2. The value of v for Sample 2 was smaller than that for Sample 1 for a given L. This suggests that the contact area is an important factor in understanding the sliding velocity.

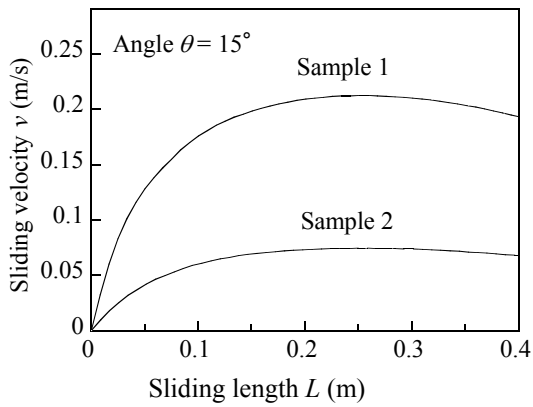

Figure 4: Sliding velocity v as a function of sliding length L ($\theta = 15°$).

Figure 5 shows two images combined to illustrate the change in the contact area due to sliding at $\theta = 15°$, where $L = 0$ m for the two samples indicates the images recorded before sliding, and $L = 0.4$ m indicates the images recorded after sliding. The diameter of the contact area before sliding (at $L = 0$ m) was ~0.4 mm for Sample 1 and ~0.5 mm for Sample 2. Their ratio was ~1.25, suggesting the validity of the Hertz contact theory given by $a_c \propto (N \cdot R_i)^{1/3}$, where a_c is the diameter of the

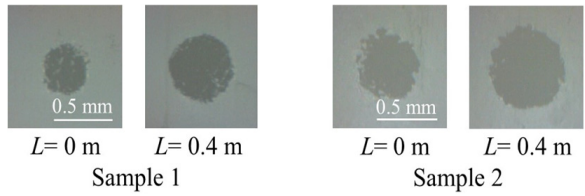

Figure 5: Change in the contact areas due to sliding (θ= 15°).

contact area, N is the contact force, and R_i is the radius of an elastic sphere on a flat substrate [25]. Thus, the ratio theoretically given is 1.26 for R_2/R_1 = 2. The contact areas for both samples increased with the sliding length, due to the wear of the Teflon spheres. The root mean square (rms) roughness of the wear surface was ~50 nm; no significant difference in the wear surface roughness was evident with respect to the original surface of the sample before sliding. Note that Sample 2 showed a larger contact area than Sample 1 did for a given L.

Figure 6 plots the average sliding velocity v^*as a function of the total sliding length L^*(= $n\,\Delta L$) at θ= 15°, where v^* is the average velocity on the sliding interval ΔL (= 0.4 m), and n is the number of the sliding repetition. v^* for both samples decreased with L^*, and Sample 2 showed smaller values than those for Sample 1 for a given L^*. The initial value of v^* was 0.24 m/s for Sample 1 and 0.12 m/s for Sample 2; their ratio was ~2.0.

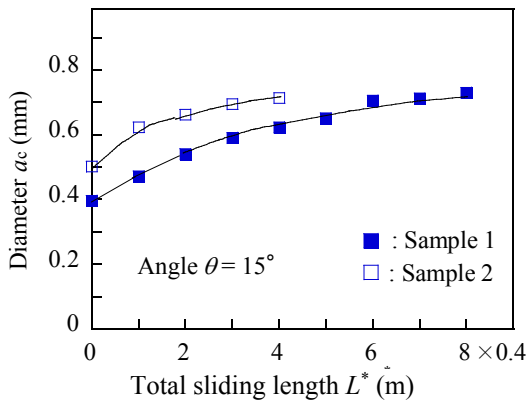

Figure 6: Diameter of contact area a_c as a function of the total sliding length L^* (θ= 15°).

Figure 7 shows the diameter of the contact area a_c as a function of L^*, where a_c is the average value of the three contact areas. a_c for both samples increased with L^*, and Sample 2 showed larger values than Sample 1 for a given L^*. As stated above, the ratio of the initial a_c values for both samples was ~1.25. This suggests that the velocity is related to the square of the contact area, because similar values were determined for the two ratios, i.e., (v_1^*/v_2^*) = 2.0 and $(A_2/A_1)^2 = (a_{c2}/a_{c1})^4$ = 2.45, different from the static friction that depends on the product of the normal stress and contact area.

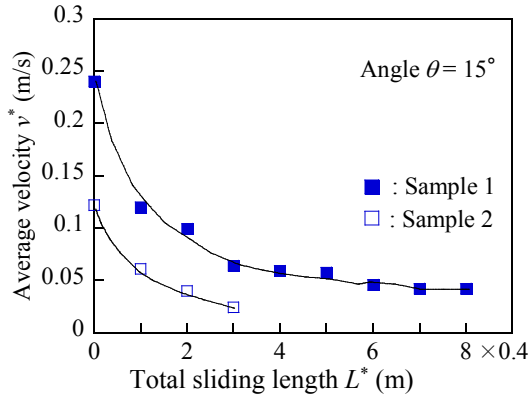

Figure 7: Average sliding velocity v^*as a function of the total sliding length L^* ($\theta = 15°$).

Figure 8 shows the average sliding velocity v^*as a function of the contact area A ($= 3/4\pi a_c^2$) for $10 < \theta < 20°$, where the results for Samples 1 and 2 are indicated with solid and open symbols, respectively. Although scattering was evident in the data, $v^*$for a given θ decreased with A, indicating that the contact area is an important factor in sliding friction. However, in order to elucidate the physical meaning of the present results, further research works are necessary. One should

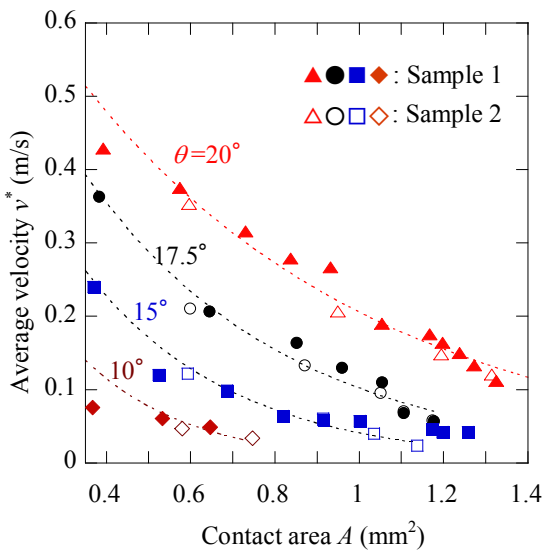

Figure 8: Average sliding velocity v^*as a function of the contact area A for inclined angles of $10 < \theta < 20°$.

be the effect of temperature on the contact area of the samples since the temperature at the interface increases during sliding. Another study to be done is the effect of wear on the sliding velocity because the wear debris can be an influential parameter in understanding the dynamic sliding friction on dry surfaces [26].

4 Conclusion

The effect of the contact area on the sliding velocity of the Teflon sample on a glass plate can be summarized into three points: (i) the sliding velocity increased in the early stages of sliding and then decreased in the later stages, (ii) the contact area increased with the sliding length due to the wear of the Teflon spheres, and (iii) the sliding velocity decreased with the contact area, indicating that the contact area plays an important role in sliding friction.

References

[1] Persson, B.N.J., *Sliding Friction: Physical Principles and Applications*, Springer-Verlag: Berlin, 1998.
[2] Kietzig, A.M., Hatzikiriakos, G. & Englezos, P., Physics of ice friction. *J. Appl. Phys.*, **107**, 081101, 2010.
[3] Goldsby, D.L. & Tullis, T.E., Flash heating leads to low frictional strength of crustal rocks at earthquake slip rates. *Science*, **334**, pp. 216-268, 2011.
[4] Lockner, D.A., Morrow, C., Moore, D. & Hickman, S., Low strength of deep San Andreas fault gouge from SAFOD core. *Nature*, **472**, pp. 82-85, 2011.
[5] Corwin, A.D. & de Boer, M.P., Effect of adhesion on dynamic and static friction in surface micromachining. *Appl. Phys. Lett.*, **84**, 2451, 2004.
[6] Gotsmann, B. & Lantz, M.A., Atomistic wear in a single asperity sliding contact. *Phys. Rev. Lett.*, **101**, 125501, 2008.
[7] Riedo, E., Gnecco, E., Bennewitz, R., Meyer, E. & Brune, H., Interaction potential and hopping dynamics governing sliding friction. *Phys. Rev. Lett.*, **91**, 084502, 2003.
[8] Tambe, N.S. & Bhushan, B., Nanoscale friction mapping. *Appl. Phys. Lett.*, **86**, 193102, 2005.
[9] Lessel, M., Loskill, P., Hausen, F., Gosvami, N.N., Bennewitz, R. & Jacobs, K., Impact of van der Waals interactions on single asperity friction. *Phys. Rev. Lett.*, **111**, 035502, 2013.
[10] Dias, R.A., Coura, P.Z. & Costa, B.V., Velocity, temperature, normal force dependence on friction: An analytical and molecular dynamics study. *Phys. Status Solidi.*, B **247**, pp. 98-103, 2010.
[11] Dieterich, J.H. & Kilgore, B.D., Direct observation of frictional contacts: New insights for state-dependent properties. *Pure and Appl. Geophys.*, **143**, pp. 283-302, 1994.
[12] Borovsky, B., Booth A. & Manlove, E., Observation of microslip dynamics at high-speed microcontacts. *Appl. Phys. Lett.*, **91**, 114101, 2007.

[13] Rubinstein, S.M., Cohen, G. & Fineberg, J., Dynamics of precursors to frictional sliding. *Phys. Rev. Lett.*, **98**, 226103, 2007.
[14] Dietzel, D., Ritter, C., Mönninghoff, T., Fuchs, H., Schirmeisen, A. & Schwarz, U.D., Frictional duality observed during nanoparticle sliding. *Phys. Rev. Lett.*, **101**, 125505, 2008.
[15] Maegawa, S., Suzuki, A. & Nakano, K., Precursors of global slip in a longitudinal line contact under non-uniform normal loading. *Tribol. Lett.*, **38**, pp. 313-323, 2010.
[16] Riedo, E., Lévy, F. & Brune, H., Kinetics of capillary condensation in nanoscopic sliding friction. *Phys. Rev. Lett.*, **88**, 185505, 2002.
[17] Reimann, P. & Evstigneev, M., Nonmonotonic velocity dependence of atomic friction. *Phys. Rev. Lett.*, **93**, 230802, 2004.
[18] Chen, J., Ratera, I., Park, J.Y. & Salmeron, M., Velocity dependence of friction and hydrogen bonding effects. *Phys. Rev. Lett.*, **96**, 236102, 2006.
[19] Li, Q., Dong, Y., Perez, D., Martini, A. & Carpick, R.W., Speed dependence of atomic stick-slip friction in optimally matched experiments and molecular dynamics simulations. *Phys. Rev. Lett*., **106**, 126101, 2011.
[20] Schirmeisen, A., Jansen, L., Hölscher, H. & Fuchs, H., Temperature dependence of point contact friction on silicon. *Appl. Phys. Lett.*, **88**, 123108, 2006.
[21] Dias, R.A., Rapini, M., Costa, B.V. & Coura, P.Z., Temperature dependent molecular dynamic simulation of friction. *Braz. J. Phys.*, **36**, pp. 741-745, 2006.
[22] Ando, Y., The effect of relative humidity on friction and pull-off forces measured on submicron-size asperity arrays. *Wear*, **238**, pp. 12-19, 2000.
[23] Merkle, A.P. & Marks, L.D., Friction in full view. *Appl. Phys. Lett.*, **90**, 064101, 2007.
[24] Arakawa, K., Effect of time derivative of contact area on dynamic friction. *Appl. Phys. Lett.*, **104**, 241603, 2014.
[25] Timoshenko, S.P. & Goodier, J.N., *Theory of Elasticity*, third ed., McGraw-Hill, Ltd., 1970.
[26] Shen, J.T., Pei, Y.T. & De Hosson, J.Th.M., Structural changes in polytetrafluoroethylene molecular chains upon sliding against steel. *J. Mater. Sci.*, **49**, pp. 1484-1493, 2014.